Beam Combiner Studies for the Magdalena Ridge Observatory Interferometer

Fabien Baron[a], David F. Buscher[a], Julien Coyne[a], Michelle J. Creech-Eakman[b], Chris A. Haniff[a], Colby A. Jurgenson[b], John S. Young[a]

[a]Cavendish Laboratory, JJ Thomson Avenue, Cambridge CB3 0HE, United Kingdom;
[b]New Mexico Institute of Mining and Technology, 801 Leroy Place, Socorro, NM 87801, USA;

ABSTRACT

We present four alternative designs for a near-infrared science beam combiner for the Magdalena Ridge Observatory Interferometer. The candidate designs considered are: (1) a four way pupil-plane combiner, fed by a "fast switchyard" that would be reconfigured at a few minute intervals to select different subsets of six input beams; (2) a four way image-plane combiner, fed by a similar fast switchyard; (3) an eight way pupil plane combiner; and (4) a six way image plane combiner. The criteria by which fully-optimised versions of the designs will be compared include: realistic signal-to-noise and imaging speed, stability and ease of alignment and calibration, cost (including detector costs), and technical and schedule risk to the MROI project.

Keywords: Interferometry, Beam combiner, MROI, Switchyard, bulk optics

1. INTRODUCTION AND BACKGROUND

The Magdalena Ridge Observatory[1–3] is a US Federally funded project being built by the New Mexico Institute of Mining and Technology (NMT) on Magdalena Ridge just west of Socorro, NM. It consists of two separate science instruments, a fast-tracking 2.4 m telescope and an optical interferometric array (MROI). The interferometric array is planned to consist of ten 1.4 m telescopes in a Y configuration, operating in the optical and near-infrared. The main participating partners in this interferometer project are NMT and the Cambridge Optical Aperture Synthesis Telescope (COAST) group at the Cavendish Laboratory in the University of Cambridge.

The MROI facility-class array is intended to be optimised strictly for model-independent imaging. In a first phase, only six telescopes will be built, and early instruments will allow science at low to medium spectral resolution in the infrared. A wide variety of targets will be observed, which should include Active Galactic Nuclei, variable stars, planetary disks and Young Stellar Objects. The most demanding case in term of sensitivity, from which is derived a limiting magnitude $H = 14$, is the AGN science mission. Beam combiners for MROI will also need to meet several other specifications, detailed in section 2 of this paper, which no existing beam combiner can currently reach. Therefore a concept study has been launched to determine possible candidate layouts for beam combiners.

Members of the MROI team at NMT have years of experience in astronomical instrumentation and interferometry, and the COAST group has recently been involved in a VLTI concept study for second generation instruments. It is with this background in mind that we have proposed the pupil and image plane combiner designs presented in section 3. Four candidate designs for a science beam combiner have been chosen. COAST and NMT groups are now performing a comparative evaluation of all of them, as explained in section 4.

Further author information:
J.C. : E-mail: jc466@mrao.cam.ac.uk, Telephone: (+44) (0)1223 337247
F.B. : E-mail: baron@mrao.cam.ac.uk, Telephone: (+44) (0)1223 766476

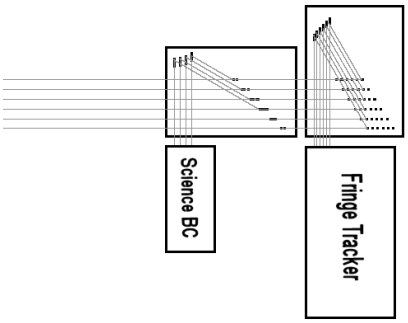

Figure 1. A science beam combiner with a 'fast switchyard' (such as the P4S or the I4S combiners) and the fringe tracker (with a 'slow switchyard'). The 'slow switchyard' reorganizes the beam to feed the fringe tracker so that consecutive beams correspond to nearest-neighbour baselines. It is rarely reconfigured (hence its name).

2. REQUIREMENTS FOR MROI COMBINERS

2.1. Instrument requirements

The beam combiner instrument itself is composed of separate science and fringe tracking combiners operating simultaneously. This approach allows to clearly distinguish the specific requirements of each combiner and then to optimise each of them for their own tasks.

Figure 1 presents a schematic layout of both combiners. The science combiner will acquire data in the J ($1.2 - 1.4\mu$m), H ($1.5 - 1.8\mu$m) and K ($2.2 - 2.5\mu$m) spectral bands (only one band at a time), while the fringe tracker will be limited to H and K bands. It should be noted that both combiners will never work in the same spectral band at the same time. A set of dichroics reflects the beams (in the science spectral band) toward the science combiner. In the fringe tracking spectral band, the beams travel through the dichroics to the fringe tracker.

In general good dichroic designs always reflect shorter wavelengths. Therefore the science combiner will be located before the fringe tracker : when science will be done in J band (respectively H band), the fringe tracker will operate in the H band (K band respectively). Special dichroics which reflect the K band and transmit the H band to the fringe tracker will be used to do science in the K band. For the same reason, the future visible science combiner (part of a later phase at MROI) will be located before the infrared science combiner : fringe tracking will (most likely) be done in the H band when the visible combiner will operate. As several possible combinations of infrared bands are possible for fringe tracking and science, care must be taken to match internal optical paths to take inter-band dispersion and internal drifts into account.

The interferometric instrumentation should handle six telescopes in a first phase, and up to ten in a later phase. Consequently beam combiner candidates only need to be able to make use of six input beams for now. The fringe tracking will allow full use of all available beams for direct combination, but the science combiner may not actually need to do a direct 6 way combination. In this case a fast switchyard can then be used to select a smaller amount of beams, for example 4 from 6, and then feed them to a 4-way combiner only.

Other top level requirements for the beam combiners include compatibility with the (indoor) beam size of 13 mm for MROI (18 mm clear aperture to allow for diffraction), as well as with the planned locations and sizes of the optical tables inside the facility.

2.2. Fringe Tracking Combiner

The fringe tracking scheme would need co-phasing and phase referencing (dual feed) for the measured phase to be a useful quantity. However prohibitive costs prevent us from taking this approach. Hence we chose to measure closure phase, and to use fringe tracking in order to improve the signal-to-noise ratio. The selected approach is

to use hardware coherencing (group delay tracking) and an optional software cophasing for bright targets. As the science targets are resolved, baseline and wavelength bootstrapping will be used.

The fringe tracker should be able to operate in the H and K spectral band (one at a time), and the group delay tracking will be active on about five spectral channels across the selected waveband. The best sensitivity will be obtained in the H band, the required limiting sensitivity being defined by the AGN science mission as H=14.

The fringe tracking combiner will use a nearest-neigbour pairwise combination approach, either in the pupil or in the image plane. Thus it should be able to track on all nearest-neighbour baselines simultaneously, effectively five baselines for the nominal six telescopes. A fringe tracker measuring other baselines would have also been possible, but the resulting signal to noise ratio penalty under this approach is unappealing. Finally the fringe tracking combiner should be easily reconfigurable in order to handle unavailable telescopes. The description of the downselected fringe tracking combiner candidate is beyond the scope of this paper though, and will not be discussed further.

2.3. Science Combiner

The science combiner should acquire visibilities and closure phases in the J, H and K spectral bands (one band at a time), in a low or medium spectral resolution mode ($R = 30$ or $R = 300$). In the future a case for high resolution mode ($R > 1000$) may eventually emerge and designs should take this possibility into account.

As for the fringe tracking combiners, the limiting sensitivity is also given by the AGN science case : in the low resolution mode, a signal-to-noise ratio greater than 2 should be achievable on an object of magnitude K=13 within 100 seconds.

The requirements on the calibration have been estimated as 2% rms on the squared visibility V^2, and 0.8^o rms on the closure phases, both on bright targets. The science combiner also has to respect the incoming polarisation of the beams.

Finally, in the case where a fast switchyard (see 3.2) is part of the design it should allow access to all baselines and independent closure triangles within a few minutes.

3. CANDIDATE COMBINERS

3.1. Concepts : P4S, P8, I4S, I6

Four candidate science beam combiners are being considered :

- 4-way pupil plane fed by fast switchyard (**P4S**). The fast switchyard selects 4 of the 6 input beams to be sent to the science combiner.
- 4-way image plane fed by fast switchyard (**I4S**). As for the combiner P4S, the switchyard is 6-way-in 4-way-out.
- 8-way (6 inputs used) pupil plane (**P8**). Two very simple 2-position internal switchyards select the baselines/triangles.
- 6-way image plane.

3.2. Fast Switchyards (P4S, I4S).

The role of a fast switchyard is to select a subset of the input beams, reorganise them and send them towards the beam combiner, in the science spectral band (see figure 2).

The switch from one optical layout of the switchyard to another (reconfiguration of the switchyard) is made by moving the optical elements (dichroics and mirrors) on their slides. Since it has to be reconfigurable in about $10 - 30$ seconds, each mirror and dichroic is mounted on a mechanical linear slide.

The slides should have a high repeatability to ensure the switchyard can be reconfigured quickly without the need to realign it, and without the need for a dedicated metrology system.

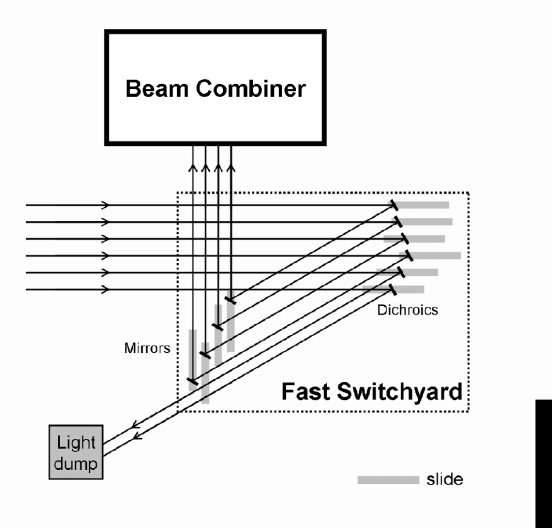

Figure 2. Fast switchyard (in the science spectral band) : 4 input beams (out of the 6 available) are selected and sent to the beam combiner. The beam pitches and the angles the beams make with the planes where all the beams have the same phase are different for the input beams and the output beams. The 2 non-selected beams are stopped outside of the switchyard.

A science combiner should be able to measure all the accessible visibilities (on baselines : interferences between 2 beams) and closure phases (on triangles : interferences between 3 beams).

Since the size of the slides will drive the cost of the switchyard, the opto-mechanical layout of the fast switchyard is optimised in order to minimise the length of the slides, while still allowing enough switchyard configurations to measure all visibilities and closure phases.

Typically, beam combiners (n_{in} input beams) measure all the visibilities and closure phases at the same time. A beam combiner (n_{out} input beams, with $n_{out} < n_{in}$) with a fast switchyard measures only a subset of the visibilities and closure phases at once. However a given signal to noise ratio on those measurements is reached much faster than with a conventional beam combiner. Reconfiguring the switchyard allows the beam combiner to eventually measure all the visibilities and closure phases.

The reconfigurations of the fast switchyard should be automated : it should be fast (about $10-30$ seconds, to be compared with the 30 seconds $-$ 3 minutes for data acquisition in a given configuration), and the switchyard will be reconfigured very often during an observation run (every 30 seconds $-$ 10 minutes, depending on the observing strategy).

Typically the fast switchyard should be reconfigured several times per cycle Calibrator/Target (probably about $4-6$ times with the P4S or the I4S combiner). The shortest interval between reconfigurations is set by the duration of the data acquisition in a given configuration : 30 seconds $-$ 3 minutes.

3.3. Pupil Plane

In the pupil plane scheme, a time modulated optical path delay is added to each beam. The collimated beams are then combined with beam-splitters. The measured intensity of an output beam is time dependent, the frequency of the oscillations depending on the pair of input beams considered. The visibility for each pair of input beams and the closure phases for each group of three input beams can be straightforwardly derived from the measured time variations of the output beams intensities.

The optical designs rely on bulk optics : the beam combiners are only based on glass slabs. They work in the J, H and K bands and have a very high throughput. A prototype for this type of technology has already been built and tested at COAST.[4]

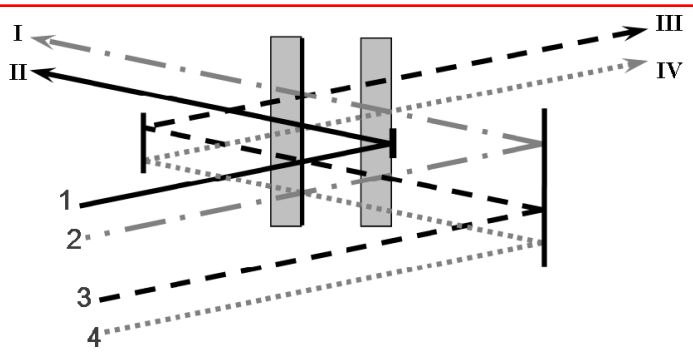

Figure 3. P4 beam combiner : bulk-optics all-on-one beam combiner.

3.3.1. P4S

The candidate science combiner P4S is a 4-way pupil plane beam combiner with a fast switchyard (see figure 3).

The fast switchyard is used to select 4 of the 6 input beams to be sent to the science combiner. Different sets of 4 beams can be selected by reconfiguring the switchyard so that, in principle, the 4-way science combiner can measure (sequentially) all of the 15 visibilities and 20 closure phases that are possible with a 6-element array. To measure all the visibilities and closure phases, 5 successive switchyard configurations are necessary (3 configurations if only visibilities are of interest).

The beam combination is performed using 50:50 beam-splitter coating on glass slabs. The beam combination is of the type all-on-one : interference between all pairs of beams selected by the switchyard is present in every output.

Without anti-reflection coatings on the surfaces of the slabs, ghost beams (parasite reflections on the surfaces of the slabs) can significantly decrease the performances of the combiner if not properly taken into account during the design. To minimise the visibility losses, the layout would have to be at least 1000×500 mm^2. It should also be noted that anti-reflection coatings allow a significantly more compact footprint : 450×250 mm^2.

3.3.2. P8

The candidate combiner P8 is a 8-way combiner where only 6 inputs are used. Two very simple 2-position internal switchyards select the baselines/triangles. Reconfiguring the internal switchyards gives access to all of the 15 visibilities that can be measured with a 6-element array. This beam combiner can also be used with a 8-element array without any modification.

With 8 input beams, each output beam is a combination of 4 input beams (see figure 4). Hence the requirements on the path modulators are not quite as demanding as for an all-on-one 8 way pupil plane combiner, the highest path modulation frequency is significantly smaller with the P8 design.

Again, anti-reflection coatings minimise the visibility losses due to ghost beams, and therefore the footprint can be kept to a minimum : 1000×250 mm^2 (overall footprint of the beam combiner + internal switchyards : 1300×800 mm^2). Without such coatings, it would most probably be quite difficult to fit the P8 combiner inside the beam combining facility.

3.3.3. Optics

The optical designs for the P4S and P8 beam combiners are based on several glass slabs. Three types of opto-mechanical designs are being considered :

- Independent : each glass slab can be positioned independently of the other slabs. Misalignments (thermal drift...) might require frequent realignments. However this design has less degrees of freedom than a layout with separate optical components, and is therefore less prone to misalignement.

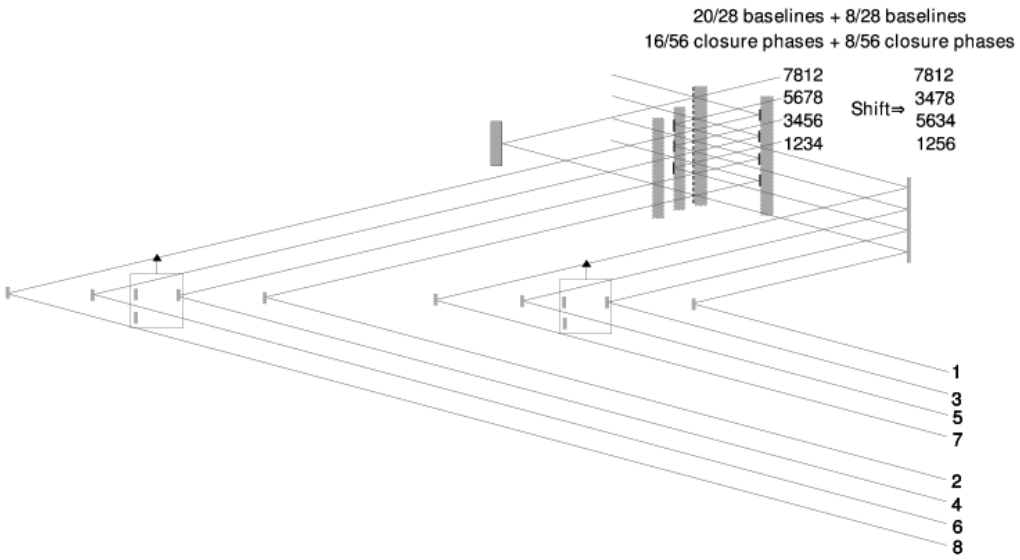

Figure 4. P8 combiner : configuration with 8 beams. The two internal switchyard allow to switch between 2 configurations. In the first configuration a subset of the baselines and closure phases is acquired, while in the second configuration another subset is measured. The layout is the same with 6 input beams : the only difference would that 2 of the input beams on the figure would not be used.

- Glass spacers : the slabs are contacted with glass spacers. Misalignment due to thermal drift should be negligible.
- Silicon bonding : the slabs are glued (via silicon bonding) on a glass substrate. Again, misalignment due to thermal drift should be negligible.

The Beam Combining Facility will be thermally controlled to within 0.1^o Celsius.[5] However long-term temperature fluctuation might be slightly larger. Therefore beam combiners insensitive to thermal drift would not need to be realigned as often as conventional designs.

The high transparency of Infrasil over the J,H and K bands would be perfectly suited for the glass slabs, while the low thermal expansion of Zerodur would be ideal for the glass spacers.

The slabs should have a thickness precise to the micron, and the surfaces of the slabs should be parallel to a few arcseconds (for the P4S combiner). This angle is ten times smaller for the slabs of the P8 combiner.

The requirements for the slabs are about 5 times more demanding if spacers are used : any non-nominal thickness of a slab or non-nominal angle between surfaces can not be compensated for when the distances and angles between the slabs are determined by the glass spacers.

3.4. Image Plane combiners : I4S and I6

Contrary to the pupil plane, for both image plane science combiners, I4S and I6, the beam combination and spectroscopy are realized simultaneously. The afocal beams are combined inside a cryostat, where the dispersed spatial fringes are formed on a Focal Plane Array (FPA).

The beam combining part of the image plane combiners is constrained by two requirements : the fringe sampling and the PSF size along the spectral dispersion axis. Both are responsible for the anamorphosis factor, the ratio of the focal lengths along the axes parallel and perpendicular to fringes. As a general rule, the greater the anamorphosis factor is, the larger the footprint of the combiner is, meaning increased costs. Consequently additional efforts were made to reduce the dewar size as much as possible.

To achieve correct fringe sampling, at least 4 pixels are needed across all fringes, as fewer samples lead to an unacceptable visibility loss. This requirement translates into 4 pixels in the highest frequency fringes, corresponding to the longest baselines. The beam configurations in input are linear and non-redundant configurations. The maximum baseline for such configurations corresponds to the distance between opposite side beams (plus the beam diameter width). As the optic mounts are unfortunately larger (40 mm) than the beam width (13 mm), the actual configuration is not the most compact of all possible non redundant configurations. Thus the actual maximum baselines are respectively $B = 192$ mm and $B = 388$ mm for four and six beams. The beam diameter stays fixed at 13 mm (clear aperture 18 mm), meaning relatively high B/D ratios and therefore high anamorphism.

Along the dispersion axis, the size of the undispersed PSF on the FPA corresponding to one spectral resolution element should be small enough not to impact the measurement of another one. Assuming one pixel per spectral resolution element, a reasonable choice is that the diameter of the first black ring of the Airy pattern of one beam should not be larger than one pixel.

When considering the whole beam combiner, calculations done with the above requirements actually lead to very large anamorphosis factors of about 310 for the I4 combiner and about 620 for the I6 combiner. The conventional solution to implement moderate anamorphosis is to use an afocal combination of two cylindrical mirrors with the ratio of their focal lengths equal to the anamorphosis ratio. While this works perfectly for three beam recombination in a single band (see AMBER concept study[6]) for which the anamorphosis ratio is about a few tens, such a design is inadequate for our purpose. Thus a three mirrors design was selected as a compromise between simplicity, cost (a single additional mirror) and compactness. The choice of focal lengths was constrained both by available realistic optical specifications, and the need for a dewar as small as possible. The only possible drawback to this approach is the absence of a pupil plane inside the dewar, which might make alignment more difficult.

Finally calculations were done to derive all acceptable sets of focal lengths, then the most compact design was chosen. Figure 5 presents the final layouts of both I4S and I6 combiners. The difference between both is rooted in the large increase of the size of the input beam configuration when going from 4 to 6 beams. Consequently the sizes of all elements – the optical ones, but the dewar as well – scale up. It is obviously also more difficult to constrain aberrations for a 6 beam combiner, due to larger off-axis distances.

3.5. Spectrographs for pupil plane and image plane

Spectroscopy in the image plane combiner is achieved by dispersing the anamorphic beams then recombining them on the FPA as a pattern of dispersed fringes.

The spectrograph layout for pupil plane combiners is somewhat simpler. Each single combined and afocal beam is focused to a cold spatial filter and then recollimated. It travels through a cold stop (in the pupil plane), then is chromatically dispersed and focused on a Focal Plane Array (FPA). As each output of the combiner requires a corresponding spectrograph, to reduce the number of FPAs needed (and thus their cost), multiplexing several beams on the same detector is planned (see for example figure 6). For the P8 combiner, at least four output beams are sent to spectrographs. For the P4 combiner actually only two output beams need to be analysed with a spectrograph. With four spectrographs, the measurements are redundant. However the more spectrographs that are used, the faster the visibilities and closure phases would be acquired.

Dispersive elements for the pupil or image plane spectrographs can be gratings or grisms, used at their first order of dispersion. All these elements – which will have to be usable in a cryogenic environment – will be mounted on a wheel, allowing rapid selection of the desired resolution from a low resolution mode ($R = 30$) and a medium resolution mode ($R = 300$).

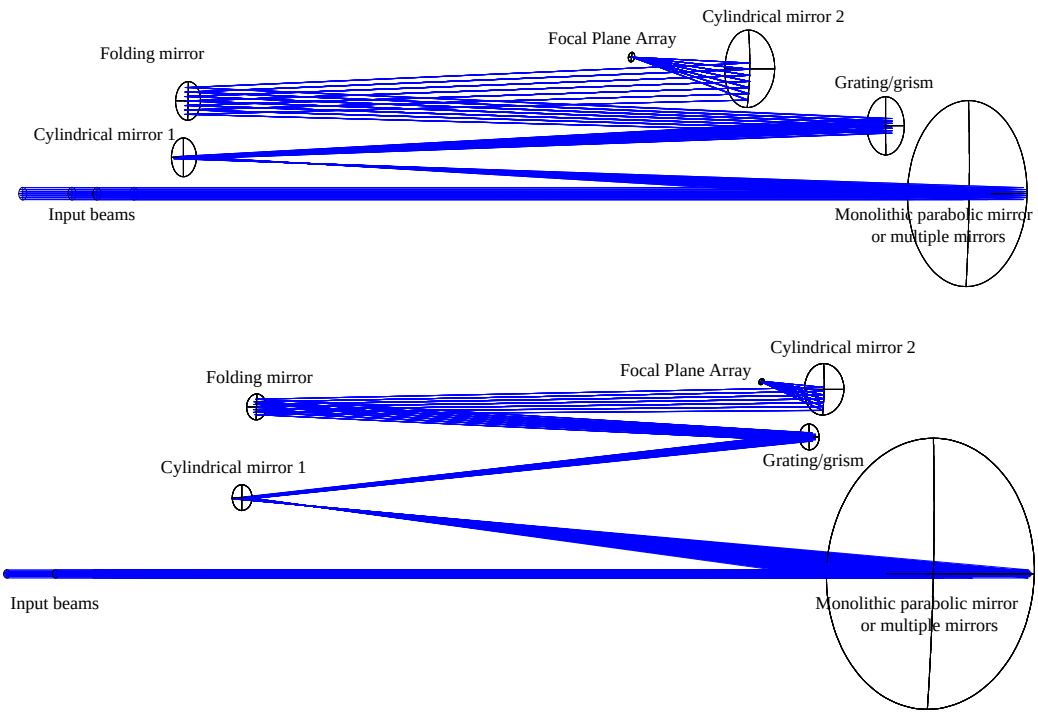

Figure 5. The I4 (top) and I6 (bottom) image plane combiners.

For a focal plane combiner, to achieve a spectral resolution R in J, H and K bands, it can be shown that about $0.2R$ pixels are required across the FPA. Thus for the medium resolution mode at least a 64×64 pixels FPA is needed. But in fact 256×256 pixels arrays are currently (Spring 2006) planned, leaving a fair margin of manoeuvre. Nevertheless, to access even higher resolution modes in the future, the FPA may have to be changed or a restricted wavelength range will have to be selected.

The dewar containing the detector device is also a more-or-less integral part of the combiner, as it is imperative that the detector should not see room temperature surfaces for wavelengths greater than 2μm. The sky background must be limited too, which can also be achieved by the dewar cold stop used as a spatial filter for wavefront cleaning. The dewar volume has been optimised during the optical design phase to keep it as small as possible. This allows to preserve cooling efficiency and easier cryogenic maintenance.

Finally, another important feature of the spectrograph must also be its ability to be easily adjusted when switching the operating dispersion mode and/or the current waveband. Note that the need to change dispersing element may arise when switching waveband even if not changing spectral resolution. In all those cases, only the last mirror and FPA should required realignment.

4. EVALUATION OF COMBINERS

We present here the main criteria on which our ongoing evaluation of beam combiner concepts are based.

4.1. Realistic signal-to-noise

An important evaluation criterion for both the fringe tracking and science beam combiners is the signal-to-noise achievable for fringe measurement. The signal-to-noise in the fringe tracker sets the limiting sensitivity for the interferometer: if there is sufficient signal for group-delay tracking then arbitrarily-long (incoherent) integration times (perhaps spread over multiple nights, at the same sidereal time) can be used to build up signal-to-noise in the science combiner.

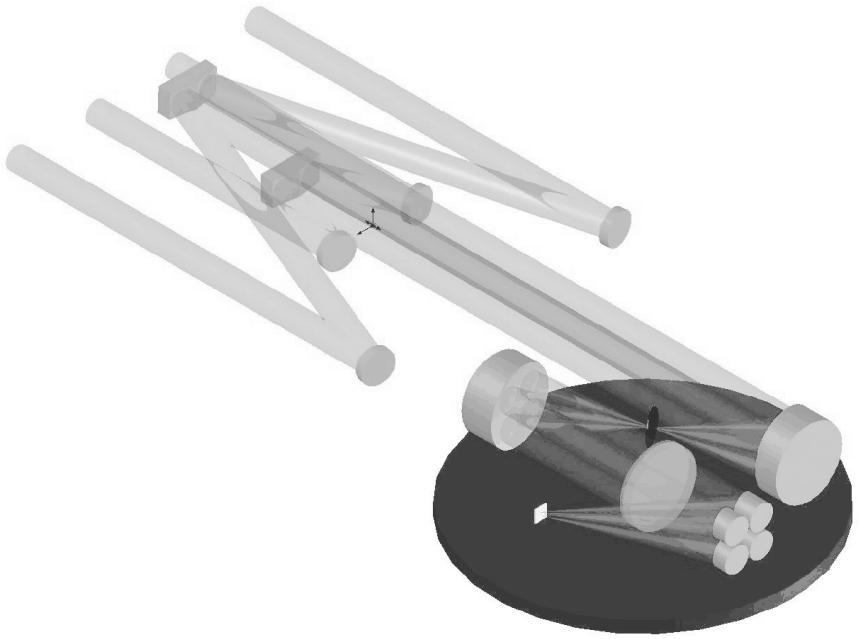

Figure 6. Fringe tracking combiner spectrograph : 4 beams multiplexed on a single detector. Work on adapting this multiplexing scheme to the science spectrograph layout is ongoing.

Provided the fringe tracker can operate, the signal-to-noise realised by the science combiner then determines how much observing time is required to map a target to a certain dynamic range in the reconstructed image — see Sec. 4.2 for more details. To allow useful science on a sample of ~ 100 Active Galactic Nuclei, the minimal requirement is that a signal-to-noise above 2 be reached in 100 seconds on a $K = 13$ target.

For the science combiner, the appropriate expression for the fringe signal-to-noise per coherent integration (typically a few times t_0) is

$$\mathrm{SNR} = \frac{\langle V^2 \rangle N_{\mathrm{source}}^2}{\sqrt{(N_{\mathrm{source}} + N_{\mathrm{background}})^2 + 2(N_{\mathrm{source}} + N_{\mathrm{background}})N_{\mathrm{source}}^2 \langle V^2 \rangle + 2n_{\mathrm{pixel}}^2 \sigma^4}}, \quad (1)$$

where $\langle V^2 \rangle$ is the mean fringe visibility, N_{source} is the number of photons detected from the astronomical target during the coherent integration, $N_{\mathrm{background}}$ is the number of thermal background (sky plus instrument) photons detected, n_{pixel} is the number of detector reads made, and σ is the detector noise per read.

It can be seen that the signal-to-noise thus depends on:

1. Intrinsic visibility of target
2. Assumed seeing conditions (determines wavefront error due to atmosphere)
3. Wavefront error due to the interferometer "infrastructure" (Unit Telescopes, beam relay system, delay lines etc.)
4. Throughput of the interferometer infrastructure
5. Visibility losses due to fringe-tracking errors

6. Beam combiner architecture — determines visibility and fraction of input light at each combiner output
7. Fringe encoding scheme (determines n_{pixel}) and detector read noise
8. Wavefront error due to the beam combining instrument
9. Throughput of the beam combining instrument including spatial filters, spectrograph and any fast switchyard
10. Thermal background seen by the detector

We are aiming to calculate signal-to-noise values that are meaningful in the absolute sense (in order to assess the extent to which the science mission can be fulfilled) and also provide a valid comparison of the various candidate combiner designs. To realise the latter aim, it is important to base the calculations on fleshed out, optimised optical designs. This is because the performances of "ideal" combiners with the candidate architectures (i.e. only accounting for items 6 and 7 in the above list) only differ by small factors, which can be overwhelmed by the cumulative effect of implementational details such as:

- Number of surfaces: e.g. P4S involves significantly more surfaces than I6 because of the need to incorporate a fast switchyard, path modulators, and optics to multiplex multiple combiner outputs onto a single detector
- Choice of spatial filtering technology: we may select fibres for some combiner candidates but pinholes for others
- Alignment/assembly errors (for example, assembly errors may lead to significant visibility loss in P4S and P8)
- Decisions about how much crosstalk between baselines can be tolerated. This depends on the observing strategy and whether analysis techniques such as those described by Thorsteinsson & Buscher[7] are adopted.

4.2. Imaging speed

The dynamic range of images reconstructed from the visibility amplitude and closure phase measurements will depend on the number of data points and their random and systematic errors.

The dynamic range expected in a map derived from n visibility data $A\exp(i\phi)$ can in general be described by the approximate formula:

$$\text{Dynamic range} \approx \frac{\sqrt{n}}{\sqrt{(\delta A/A)^2 + \delta\phi^2}}, \tag{2}$$

where δA and $\delta\phi$ are the visibility amplitude and phase errors respectively. The visibility phase error to use in this formula can be derived from the closure phase error given certain assumptions.

The dynamic range that MROI will achieve thus depends on:

- Instantaneous science combiner signal-to-noise, calculated as in Sec. 4.1
- Overheads for calibration (star switching etc.)
- For P8/P4S/I4S, the number of switchyard reconfigurations required
- For P8/P4S/I4S, overheads for switchyard reconfiguration

The switchyard reconfiguration time must be comparable to or less than the on-source integration time for P8/P4S/I4S to achieve a competitive imaging speed. We intend to compare imaging speeds for the candidate science combiners once results from the slide tests (see section 4.3.3) are available.

4.3. Calibration and stability issues

4.3.1. Stability

To compare the stability and ease of alignment of the candidate combiners, several points should be considered :

- The number of extra optical elements required for aligning the combiner (such as an additional reference light source). It is usually a reasonable indicator for the cost, complexity and mean time between failure.
- Duration of the alignment process.
- Repeatability of the switchyard (for the P4S, I4S and P8 (internal)).
- Mechanical stability of the beam combiner and spectrograph(s) : thermal drifts...

The time spent per night and the required frequency of the alignment process can then be directly derived.

4.3.2. Calibration

Amongst the several calibration processes necessary to obtain science data with a beam combiner :

- Cycle target star - reference star. To conform to the requirements (2% rms on the squared visibilities and 0.8^o rms on the closure phase), the interferometer will have to switch several times between the target star and a bright and well-known reference star in the same patch of the sky. The number of cycles target star - reference star to obtain a set of calibrated squared visibilities and closure phases might not be the same for all the beam combiner (depending on the performance of the switchyard, it might be required to switch to the reference star after each reconfiguration).
- Beam throughput. The optical designs do not include any photometric outputs. Therefore the throughput for each beam will have to be calibrated from time to time during the night.
- Slide look-up table. If only the repeatability of the slides (but not the position and attitude) conform to the specifications, a look-up table of the corrections to apply to the optical elements on the slides will have to be built and calibrated from time to time.

The frequency, the duration and the complexity of those calibrations will be taken into account when selecting the best candidate combiner.

4.3.3. Slide tests

The requirements for the slides for the fast switchyards (for the candidate combiners P4S and I4S) have been derived with a specifically developed ray-tracing program : about a micron in position (on all three axes) and about half a arcsecond in pitch, yaw and roll.

Those requirements are rather stringent. However they only apply to the repeatability of the slides : if the position and attitude of the slides can not conform to those specifications, the requirements can be enforced with a look-up table of the corrections to apply to each optical element on the slides, providing the repeatability is better than the requirements.

The test of potentially suitable slides will be organised in two phases. First, the tip/tilt of a mirror mounted on each test slide will be tested along the course of the slide. Then for the most promising types of slide, a simplified fast switchyard layout (with only two slides) will be built. The overall OPD and tip/tilt will then be monitored as the mirrors travel on both slides.

4.4. Cost, Technical and Schedule risks

The total cost of the beam combiner device is principally determined by the costs of the detector, the dewar and the glass (in the pupil plane combiner case).

Technical risks include the glass procurement (pupil plane), FPA requirements (mostly for image plane combiners), and the slides (for combiners with a switchyard).

The main items susceptible to alter the schedule are the availability of custom cylindrical mirrors (image plane) or of the glass for slabs (pupil plane) are the most important risks for this item.

5. CONCLUSION AND PROSPECTS

MROI requirements for infrared instruments are quite demanding. Four beam combiners have been designed : a four way pupil plane combiner fed by a fast switchyard, a four way image plane combiner also fed by a fast switchyard, an eight way pupil plane combiner and a six way image plane combiner. They all work in the J, H and K bands and have a very high throughput. The comparison of the fully-optimised candidate beam combiners is ongoing and is based on : realistic signal-to-noise, imaging speed, calibration, stability and the cost, technical and schedule risks.

We expect to finish the evaluation of the science beam combiners in July 2006. First closure phase is predicted in August 2008. Six telescopes should be on site by the end of 2009.

ACKNOWLEDGMENTS

The Cambridge team acknowledges support provided by the Particle Physics and Astronomy Research Council for their ongoing research.

Magdalena Ridge Observatory (MRO) is funded by Agreement No. N00173-01-2-C902 with the Naval Research Laboratory (NRL). MRO Interferometer is hosted by New Mexico Institute of Mining and Technology (NMT) at Socorro, NM, USA, in collaboration with the University of Cambridge (UK).

REFERENCES

1. M. J. Creech-Eakman and Magdalena Ridge Observatory Interferometer Team, "Magdalena Ridge Observatory Interferometer Science Mission and Design Requirements," *American Astronomical Society Meeting Abstracts* **207**, p. 14, Dec. 2005.
2. M. J. Creech-Eakman, D. F. Buscher, C. A. Haniff, and V. D. Romero, "The Magdalena Ridge Observatory Interferometer: a fully optimized aperture synthesis array for imaging," in *New Frontiers in Stellar Interferometry, Proceedings of SPIE Volume 5491. Edited by Wesley A. Traub. Bellingham, WA: The International Society for Optical Engineering, 2004., p.405*, W. A. Traub, ed., p. 405, Oct. 2004.
3. M. J. Creech-Eakman, D. Buscher, M. Chang, C. Haniff, P. Howell, A. Jorgensen, B. Laubscher, G. Loos, V. Romero, M. Sirota, S. Teare, D. Voelz, and D. Westpfahl, "The Magdalena Ridge Optical Interferometer and its Science Drivers," *American Astronomical Society Meeting Abstracts* **203**, p. 03, Dec. 2003.
4. C. A. Haniff, J. E. Baldwin, A. G. Basden, N. A. Bharmal, R. C. Boysen, D. F. Buscher, J. W. Keen, C. D. Mackay, B. O'Donovan, E. B. Seneta, H. Thorsteinsson, N. D. Thureau, R. N. Tubbs, P. J. Warner, D. M. Wilson, and J. S. Young, "COAST: recent technology and developments," in *New Frontiers in Stellar Interferometry, Proceedings of SPIE Volume 5491. Edited by Wesley A. Traub. Bellingham, WA: The International Society for Optical Engineering, 2004., p.511*, W. A. Traub, ed., p. 511, Oct. 2004.
5. M. J. Creech-Eakman, D. F. Buscher, T. A. Coleman, C. A. Haniff, C. A. Jurgenson, J. E. Kern, D. A. Klinglesmith III, C. B. Parameswariah, V. D. Romero, A. Shtromberg, D. J. Westpfahl, and J. S. Young, "Magdalena Ridge Observatory Interferometer: Status Update," in *these SPIE proceedings, paper number 70*, 2006.
6. S. Robbe-Dubois, P. Antonelli, U. Beckmann, Y. Bresson, S. Gennari, S. Lagarde, F. Lisi, F. Malbet, G. Martinot-Lagarde, Y. Rabbia, S. Rebattu, F. Reynaud, K. Rousselet-Perraut, and R. G. Petrov, "AMBER: optical design and expected performance," in *Proc. SPIE Vol. 4006, p. 224-232, Interferometry in Optical Astronomy*, P. J. Lena and A. Quirrenbach, eds., pp. 224–232, July 2000.
7. H. Thorsteinsson and D. F. Buscher, "General fringe decomposition and statistical bias correction in optical interferometry," in *New Frontiers in Stellar Interferometry, Proceedings of SPIE Volume 5491. Edited by Wesley A. Traub. Bellingham, WA: The International Society for Optical Engineering, 2004., p.1498*, W. A. Traub, ed., p. 1498, Oct. 2004.